

# Kinetics of Demixing and Remixing in Poly(*N*-isopropylacrylamide)/Water Studied by Modulated Temperature DSC

Kurt Van Durme, Guy Van Assche, and Bruno Van Mele\*

Department of Physical Chemistry and Polymer Science-FYSC (TW),  
Vrije Universiteit Brussel, Belgium

Received July 26, 2004

**ABSTRACT:** The heat capacity signal from modulated temperature DSC can be used to measure the onset of phase separation in aqueous poly(*N*-isopropylacrylamide) (PNIPAM) solutions, showing a type II LCST demixing behavior. Quasi-isothermal measurements through the phase transition show large excess contributions in the (apparent) heat capacity, caused by demixing and remixing heat effects on the time scale of the modulation. These excess contributions and their time-dependent evolution are useful to describe the kinetics of phase separation and to follow the related morphology development. Partial vitrification of the polymer-rich phase slows down the remixing kinetics.

## Introduction

Poly(*N*-isopropylacrylamide) (PNIPAM)/water mixtures are known to exhibit demixing at physiological temperatures, which can be interesting toward applications like controlled drug release<sup>1</sup> and thermoresponsive membranes.<sup>2,3</sup> The phase separation behavior of aqueous PNIPAM solutions and hydrogels is characterized by a lower critical solution temperature (LCST), which has been thoroughly investigated by a wide variety of experimental techniques, especially in dilute conditions. Dynamic light scattering was used to monitor the coil-to-globule transition for PNIPAM single chains.<sup>4–6</sup> The driving force for this coil-to-globule transition is associated with the temperature-dependent molecular interactions, mainly hydrogen bonding and hydrophobic association.<sup>7</sup> Attenuated total reflection (ATR)/Fourier transform infrared (FTIR)<sup>8,9</sup> and nuclear magnetic resonance (NMR)<sup>10</sup> show that below the LCST the intermolecular hydrogen bonding between PNIPAM and water is predominant. Above the demixing temperature, however, hydrophobic interactions between the polymer chains are promoted. This aggregation behavior has been studied by turbidimetry or ultraviolet/visible (UV/VIS) spectroscopy.<sup>11</sup> The temperature at which demixing sets in is determined as the initial decrease in transmitted light and is often referred to as the cloud point temperature ( $T_{cp}$ ). Differential scanning calorimetry (DSC) demonstrated an endothermic heat effect at  $T_{cp}$  caused by the breaking up of hydrogen bonds.<sup>7,11–13</sup> Within this context, Cho et al. claim that throughout the demixing process of PNIPAM/water the variation in hydrophilic and hydrophobic interactions can be differentiated by means of modulated temperature DSC (MTDSC).<sup>13</sup>

Despite the importance of understanding the phase separation mechanism for the entire composition range, the information about the state diagram of PNIPAM/water is usually limited to solutions of low polymer concentration. Berghmans et al. investigated the effect of the concentration and molecular weight on the demixing temperature.<sup>14</sup> This study indicated the type II demixing behavior, having an LCST for infinite molar mass at off-zero concentration,<sup>15</sup> in this case around 45

wt % polymer. MTDSC will be used to determine a state diagram over the entire composition range for different molecular weights of PNIPAM.

Thermoresponsive surfaces usually require a fast change from homogeneous to heterogeneous and vice versa.<sup>1</sup> Although kinetic data on demixing/remixing are very important toward applications, this information can hardly be found in the literature.<sup>16–18</sup> The correlation between demixing/remixing kinetics and partial vitrification of the formed polymer-rich phase will be studied in detail with MTDSC.

In the study of polymeric materials by means of MTDSC, kinetic thermal processes, depending on time and absolute temperature, often appear in the nonreversing heat flow, while the (specific) heat capacity is found in the reversing heat flow. In this case, the latter signal equals the average heating rate times the specific heat capacity  $c_p$  ( $J g^{-1} K^{-1}$ ), which is calculated as

$$c_p = \frac{A_{HF}}{A_T \omega} \quad (1)$$

where  $A_T \omega$  is the amplitude of the imposed modulated heating rate, with  $A_T$  the temperature modulation amplitude (K),  $\omega$  the modulation angular frequency ( $=2\pi/p$ ), and  $p$  the modulation period (s);  $A_{HF}$  is the amplitude (of the first harmonic) of the resulting modulated heat flow ( $W g^{-1}$ ). The nonreversing heat flow equals the total heat flow (the running average of the modulated signal) minus the reversing heat flow. A complete description of the extraction of the heat capacity and other MTDSC signals can be found in the literature.<sup>19–21</sup>

The straightforward deconvolution procedure turns out to be valid for the study of reaction rate and chemorheological changes in reacting polymer systems.<sup>22–24</sup> However, it no longer holds for characterizing polymer melting, temperature-induced phase separation in polymer blends and solutions, and reaction-induced phase separation in some modified epoxy–amines.<sup>16,17,25–28</sup> Heat effects, coupled with melting/crystallization<sup>25</sup> or mixing/demixing,<sup>16,17,26–28</sup> occur during a modulation cycle and thus contribute to  $A_{HF}$  in eq 1. Hence, the specific heat capacity calculated by eq 1 is termed “apparent”,  $c_p^{app}$ , to distinguish it from the baseline specific heat capacity,  $c_p^{base}$ , which is temperature-

\* Corresponding author: Fax +32-(0)2–629.32.78; Ph +32-(0)2–629.32.76 or 32.88; e-mail bvmele@vub.ac.be.

dependent. The so-called “excess” contribution,  $c_p^{\text{excess}}$ , is temperature- and time-dependent and changes with the progress of the transformation:

$$c_p^{\text{app}}(T,t) = c_p^{\text{base}}(T) + c_p^{\text{excess}}(T,t) \quad (2)$$

The ability of MTDSC to study the phase transition kinetics in quasi-isothermal conditions (average heating rate equal to zero) by means of the heat capacity signal will be explored for aqueous PNIPAM solutions.

## Experimental Section

**Materials.** Poly(*N*-isopropylacrylamide) (PNIPAM) was obtained from Polysciences Inc. (weight-average molecular weight ( $M_w$ ) = 74 000 g mol<sup>-1</sup>, polydispersity index = 3) and from Polymer Source ( $M_w$  = 186 800 g mol<sup>-1</sup>, polydispersity index = 2.6).

PNIPAM was also prepared from NIPAM monomer, Aldrich Chemical Co. Inc., as described in the literature.<sup>29</sup> The weight-average molecular weight was 18 000 g mol<sup>-1</sup>, and the polydispersity index was 4 as determined by GPC.

**Sample Preparation.** The polymers were dried under vacuum for at least 48 h at 130 °C, after which the water content was less than 0.2 wt % as determined by thermogravimetric analysis (TA Instruments TGA 2950). The glass transition of dried PNIPAM is ca. 140 °C. Starting from a 10/90 (wt/wt %) polymer/water solution, a range of compositions were prepared directly in hermetic Perkin-Elmer or Mettler aluminum pans. Samples containing more than 10 wt % polymer were prepared by evaporation of water, while those containing less than 10 wt % polymer by further dilution of the original 10/90 mixture. These samples were stored in the refrigerator for at least 1 week to obtain a homogeneous mixture. A few of the closed crucibles were perforated, and the weight loss was measured at 100 °C using TGA to check the preparation procedure (error < 1 wt %).

**Optical Microscopy Coupled with a Hot Stage (OM).** Cloud points were detected by measuring the light transmitted by thin samples between glass slides mounted in a Mettler Toledo FP82HT hot stage, which was placed in a Spectratech optical microscope (magnification ×10) equipped with a photodetector (most sensitive at a wavelength of 615 nm). Evaporation of water was avoided by using a rubber spacer between the glass slides. Temperature calibration was done with benzophenone (melting temperature,  $T_m$  = 48.1 °C) supplied by Fluka. All samples were heated (and cooled) at 1 °C min<sup>-1</sup>, using a nitrogen purge to cool below room temperature. A threshold value of 2% in the decrease of light transmittance (against 100% for the completely transparent homogeneous solution) upon heating was chosen as the cloud point temperature.

**Modulated Temperature Differential Scanning Calorimetry (MTDSC).** A first series of MTDSC measurements were performed on a TA Instruments 2920 DSC with the MDSC option and an RCS cooling accessory. Helium was used as a purge gas (25 mL min<sup>-1</sup>). Indium and cyclohexane were used for temperature calibration. The former was also used for enthalpy calibration. Standard modulation conditions were an amplitude  $A_T$  of 0.50 °C with a period  $p$  of 60 s. Heat capacity calibration was performed in standard modulation conditions with water, using the heat capacity difference between two temperatures, one above and one below the melting temperature. In this way, the most accurate measurements of heat capacity changes and “excess” contributions,  $c_p^{\text{excess}}$ , were obtained. If other modulation conditions were applied, the heat capacity was corrected by an internal calibration against the standard conditions; hence,  $c_p^{\text{base}}$  at 10 °C became constant (independent of modulation period and amplitude). Data are expressed as specific heat capacities (or changes) in J g<sup>-1</sup> K<sup>-1</sup>. Nonisothermal experiments were performed at an underlying heating rate of 1 °C min<sup>-1</sup> unless stated otherwise. Samples of 2–6 mg were introduced in hermetic Perkin-Elmer aluminum pans of 50 μL.

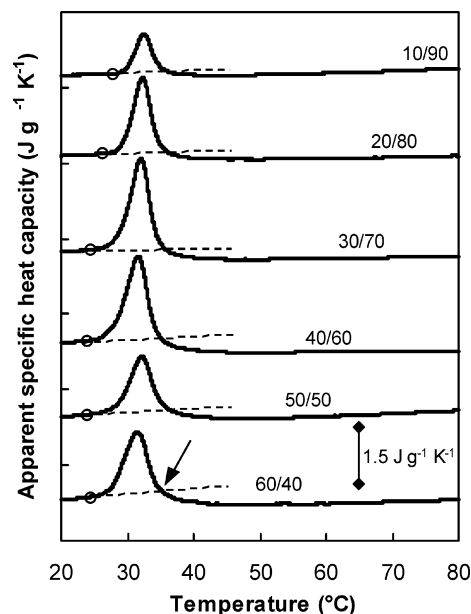


**Figure 1.**  $c_p^{\text{app}}$  during nonisothermal demixing of PNIPAM 74000/water for different compositions, demixing temperature (○). Curves are shifted vertically for clarity. Dashed line (extrapolated experimental  $c_p^{\text{base}}$ ) is a guide to the eye. Arrow indicates drop of  $c_p^{\text{app}}$  below  $c_p^{\text{base}}$  (considered as onset of partial vitrification).

A second series of MTDSC experiments were performed in hermetic Mettler aluminum pans (sample weights of 1–3 mg) on a TA Instruments Q1000 (T-zero DSC-technology) with an RCS or LNCS cooling accessory. The calibration conditions were as stated above. Nitrogen was used as a purge gas (25 mL min<sup>-1</sup>).

## Results and Discussion

**Nonisothermal Demixing of PNIPAM/Water.** Homogeneous PNIPAM/water mixtures demix upon heating; this phase separation process is accompanied by an endothermic heat effect.<sup>7,11,14</sup> Using MTDSC with the previously described standard conditions, the total demixing enthalpy is split up in two endothermic contributions. The largest part, usually more than 95%, is found in the heat capacity and as such in the reversing heat flow signal. Therefore, the former is an “apparent” specific heat capacity (calculated by eq 1) with an “excess” contribution due to reversible mixing and demixing on the time scale of the modulation<sup>16,17</sup> (see introduction and eq 2). Consequently, the endothermic enthalpy contribution in the nonreversing heat flow is usually less than 5% of the total demixing enthalpy, except for diluted samples, in which up to 15% of the heat effect is found in the nonreversing heat flow signal. Note that both heat flow contributions are endothermic in all measuring conditions, which is in contrast with the results of Cho et al.<sup>13</sup> (see also section Excess Heat Capacity: Effect of the Modulation Period).

The evolution of  $c_p^{\text{app}}$  for different compositions of PNIPAM 74000/water is shown in Figure 1. A deviation is seen from the experimental baseline specific heat capacity, indicating the start of phase separation. By using a threshold value, defined against the extrapolated experimental baseline (Figure 1, dashed lines), the demixing temperature of each sample could be obtained (Figure 1, ○). This approach was discussed in more detail for poly(vinyl methyl ether)/water<sup>16</sup> and poly(*N*-vinylcaprolactam)/water<sup>17</sup> solutions.

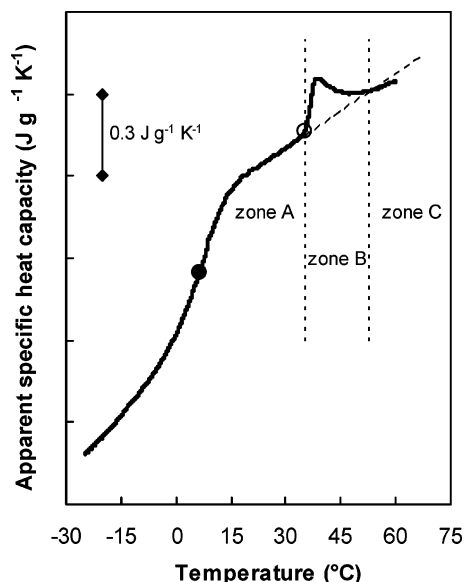


**Figure 2.**  $c_p^{\text{app}}$  during nonisothermal demixing for 80/20 PNIPAM 74000/water: demixing temperature ( $\circ$ ) and  $T_g$  ( $\bullet$ ). Dashed line (extrapolated experimental  $c_p^{\text{base}}$ ) is a guide to the eye. Zone A, homogeneous; zone B, heterogeneous without interference of vitrification; zone C, heterogeneous with partial vitrification of polymer-rich phase.

### Partial Vitrification of PNIPAM-Rich Phase.

A major benefit of using the heat capacity signal from MTDSC is the additional information beyond the demixing temperature.<sup>16,17,26,27</sup> Further heating of PNIPAM/water solutions induces partial vitrification of the formed PNIPAM-rich phase, which is seen as a drop in  $c_p^{\text{app}}$  below the extrapolated baseline specific heat capacity at ca. 35 °C, indicated by an arrow in Figure 1. The drop in  $c_p^{\text{app}}$  below  $c_p^{\text{base}}$  is not the exact onset of partial vitrification due to the effect of the superimposed  $c_p^{\text{excess}}$ .

However, the correction is small: as the partial vitrification process decreases the rate of demixing, the contribution of the phase separation heat effect to  $c_p^{\text{app}}$  ( $c_p^{\text{excess}}$ ) becomes negligible. At much higher temperatures, near the glass transition of the polymer-rich phase, the specific heat capacity again increases toward the extrapolated experimental  $c_p^{\text{base}}$  (not shown). These structural changes within the sample cannot be deduced from optical microscopy measurements in which the light transmittance drops to zero at the cloud point temperature.

Three different temperature regions can as such be defined, which is illustrated in Figure 2 for an 80/20 PNIPAM 74000/water mixture: zone A, homogeneous; zone B, heterogeneous without interference of vitrification; zone C, heterogeneous with partial vitrification of a polymer-rich phase. The conditions of phase separation (a temperature in zone B or C) will have an effect on the remixing kinetics upon cooling, as will be discussed later on. Note that for the 80/20 mixture the drop in  $c_p^{\text{app}}$  below  $c_p^{\text{base}}$  is found at ca. 52 °C, a higher temperature than for the less concentrated compositions of Figure 1 (ca. 35 °C). If only the state diagram is taken into account (Figure 3a), the onset of vitrification is expected to be constant, irrespective of the polymer concentration of the homogeneous solution. However, the higher the polymer concentration, the smaller the rates of diffusion (and thus the rate of phase separation)

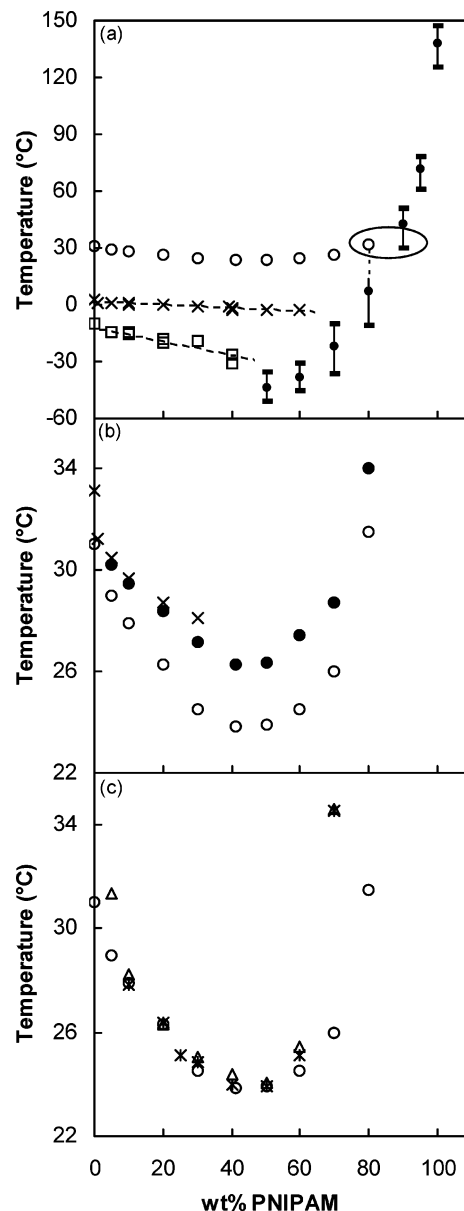


**Figure 3.** State diagram of (a) PNIPAM 74000/water, demixing curve ( $\circ$ ),  $T_g$ -composition curve ( $\bullet$ , width: I), melting ( $T_m$ :  $\times$ ) and crystallization ( $T_{cr}$ :  $\square$ ) temperature of water; (b) PNIPAM 74000/water, demixing curve: threshold in  $c_p^{\text{app}}$  0.01  $\text{J g}^{-1} \text{K}^{-1}$  ( $\circ$ ), 0.1  $\text{J g}^{-1} \text{K}^{-1}$  ( $\bullet$ ) and cloud point curve ( $\times$ ); (c) demixing curves for PNIPAM 18000/water ( $\triangle$ ), PNIPAM 74000/water ( $\circ$ ) and PNIPAM 186800/water (\*). Demixing temperatures are calculated from threshold in  $c_p^{\text{app}}$  (0.01 or 0.1  $\text{J g}^{-1} \text{K}^{-1}$ ) upon heating;  $T_g$  from  $c_p^{\text{app}}$  upon cooling;  $T_m$  and  $T_{cr}$  from the total heat flow, upon heating and cooling, respectively.

and the more the onset of partial vitrification is delayed at a constant heating rate. A similar behavior was noticed for partially miscible polymer blends<sup>26,27</sup> and for the poly(*N*-vinylcaprolactam)/water system.<sup>17</sup>

**State Diagram of PNIPAM/Water.** Figure 3a depicts the state diagram of PNIPAM 74000/water determined by MTDSC. The demixing temperature (Figure 3a,  $\circ$ ) and the glass transition temperature  $T_g$  (Figure 3a,  $\bullet$ ) are shown for different compositions.  $T_g$  could not be determined for solutions with less than 50 wt % PNIPAM because the sample could not be cooled sufficiently fast in order to prevent crystallization of water. As expected,  $T_g$  lowers with increasing water content due to the plasticizing effect of water on PNIPAM.<sup>14,17</sup>



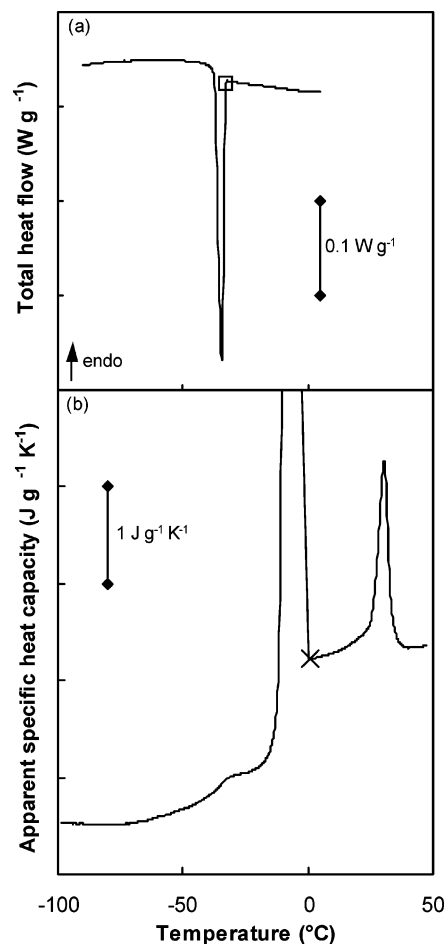


**Figure 4.** (a) Nonisothermal cooling, total heat flow: crystallization temperature of water (□) and (b) nonisothermal heating,  $c_p^{\text{app}}$ : melting temperature (×).

The width of the glass transition in Figure 3a is important because the possible interference of partial vitrification during phase separation (indicated by the oval curve) depends on the upper limit of the glass transition rather than on its average value. Berghmans et al. ruled out this interference because they only considered the average value of  $T_g$ .<sup>14</sup> The vitrification of a polymer-rich phase during phase separation was demonstrated by heating a 70/30 PNIPAM 74000/water mixture up to 60 °C (zone C), followed by a quench-cooling (using liquid nitrogen) to freeze in the formed phases. In the subsequent heating a glass transition temperature was seen at 32 °C (width of  $T_g$ : 14 °C), which nearly equals the temperature at which the apparent specific heat capacity drops below  $c_p^{\text{base}}$  (Figure 1). Note that  $T_g$  of the homogeneous 70/30 PNIPAM 74000/water mixture is -22 °C.

The melting (×) and crystallization temperature (□) of water are also shown in Figure 3a. During the crystallization process of the solvent a glassy polymer-rich phase is formed with a composition according to the  $T_g$ -composition curve of Figure 3a. This behavior is illustrated in Figure 4 for a 40/60 PNIPAM 74000/water solution. Using the total heat flow signal upon cooling (Figure 4a), it can be seen that a supercooling of 30 °C is needed to induce crystallization of water (□).<sup>14</sup> In the subsequent heating ( $c_p^{\text{app}}$  in Figure 4b), devitrification of the glassy PNIPAM-rich phase takes place at -35 °C, followed by melting of the ice crystals

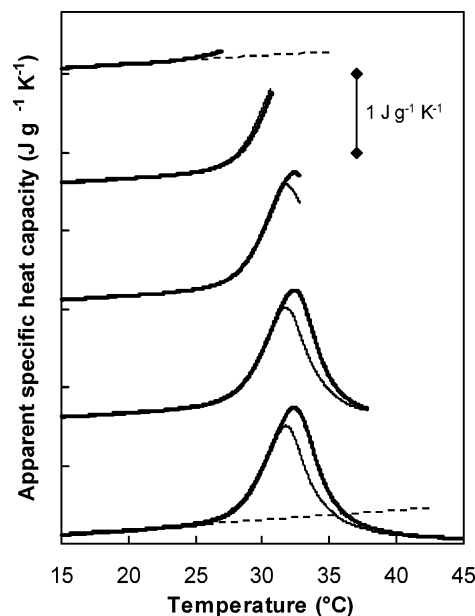


**Figure 5.**  $c_p^{\text{app}}$  during nonisothermal demixing (thick) and subsequent remixing (thin) for 50/50 PNIPAM 74000/water up to different temperatures: 27, 31, 32, 39, and 45 °C. Curves are shifted vertically for clarity. Dashed line (extrapolated experimental  $c_p^{\text{base}}$ ) is a guide to the eye.

(×) and phase separation of the partially remixed PNIPAM/water phase. Note that for this mixture the upper limit of  $T_g$  equals the crystallization temperature upon cooling. The supercooling for crystallization is increasing with the PNIPAM concentration (Figure 3a). Consequently, crystallization upon cooling is hindered for those samples containing more than 50 wt % PNIPAM due to the intersection of the crystallization and the glass transition curve (taking into account the width of  $T_g$ ) (Figure 3a). Nevertheless, melting can still be seen up to 60 wt % polymer due to cold crystallization upon heating, just above the upper limit of  $T_g$ .

Figure 3b shows the influence of the threshold value (deviation of  $c_p^{\text{app}}$  from the extrapolated baseline,  $c_p^{\text{base}}$ ) to characterize the demixing temperature. If a threshold value of 0.1 J g<sup>-1</sup> K<sup>-1</sup> is chosen, the demixing curve (●) almost coincides with the cloud point curve determined by optical microscopy (×). A more sensitive threshold value of 0.01 J g<sup>-1</sup> K<sup>-1</sup> (○), however, enables to detect the onset of phase separation up to 3 °C earlier. The latter threshold value is important to determine the temperature region of time-independent heat capacity measurements (see discussion of Figure 9).

Figure 3c shows a comparison of the type II LCST demixing behavior of PNIPAM/water mixtures for different molar masses of PNIPAM. The critical point stays at the same temperature and polymer concentration (ca. 50 wt %), independent of the polymer molar mass, in agreement with literature.<sup>14,15</sup>

**Influence of Partial Vitrification of PNIPAM-Rich Phase on Kinetics of Remixing.** The kinetics of remixing are largely influenced by the thermal history of the preceding phase separation. The temperature (zone B or C) and the duration of the demixing step are two important parameters. As an example, the remixing kinetics of a 50/50 PNIPAM 74000/water solution were studied. As long as the aqueous PNIPAM solution is kept below 32 °C,  $c_p^{\text{app}}$  on heating (Figure 5, thick) and cooling (Figure 5, thin) coincide, whereas a higher

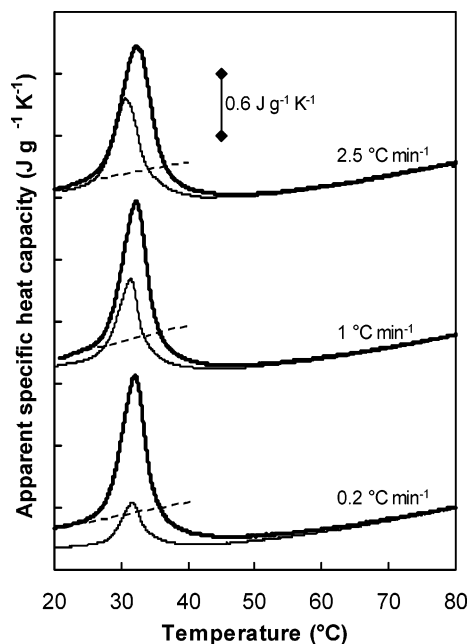


**Figure 6.**  $c_p^{\text{app}}$  during nonisothermal demixing (thick) and subsequent remixing (thin) for 50/50 PNIPAM 74000/water at different heating/cooling rates: 2.5, 1, and 0.2 °C min<sup>-1</sup>. Curves are shifted vertically for clarity. Dashed line (extrapolated experimental  $c_p^{\text{base}}$ ) is a guide to the eye.

demixing temperature results in a difference between both curves. Hence, the reversing remixing exotherm upon cooling becomes smaller than the reversing demixing endotherm. This means that the rate of remixing is slower than the rate of demixing. If the sample is initially heated to a temperature in zone C, above the onset of partial vitrification, the specific heat capacity value after partial remixing (zone A) is smaller than the initial value of the homogeneous solution. This observation is not clear in Figure 5 but becomes more pronounced by increasing the demixing time in zone C, as shown in Figure 6.

If the 50/50 PNIPAM 74000/water solution was first heated to 80 °C, the reversing heat flow and thus  $c_p^{\text{app}}$  is clearly less significant upon cooling (Figure 6, thin curves). The balance between reversing and nonreversing heat flow contributions is also different upon cooling: the nonreversing heat flow is no longer negligible and mounts up to 60% of the total heat effect.

The total demixing enthalpy equals 9.3 J g<sup>-1</sup> while the remixing enthalpy is -3.7 J g<sup>-1</sup>, using the standard heating and cooling rate of 1 °C min<sup>-1</sup>, respectively. This illustrates that the remixing process did not complete upon cooling. The longer the mixture is kept in zone C (i.e., the higher the degree of partial vitrification of the polymer-rich phase), the slower the remixing process. This behavior can be illustrated by changing the heating/cooling rate from 2.5 down to 0.2 °C min<sup>-1</sup> (Figure 6). The latter condition implies the longest residence time in zone C, causing the sample to homogenize more slowly. The total remixing enthalpy decreases from -6.8 down to -3.1 J g<sup>-1</sup>, while the difference in the value of  $c_p^{\text{app}}$  at 21 °C (zone A) is 0.002 J g<sup>-1</sup> K<sup>-1</sup> when scanning at 2.5 °C min<sup>-1</sup> and 0.250 J g<sup>-1</sup> K<sup>-1</sup> when cooling at 0.2 °C min<sup>-1</sup>.

If the partially vitrified heterogeneous mixture is subsequently kept at a temperature in the homogeneous region (zone A),  $c_p^{\text{app}}$  again increases toward the base-

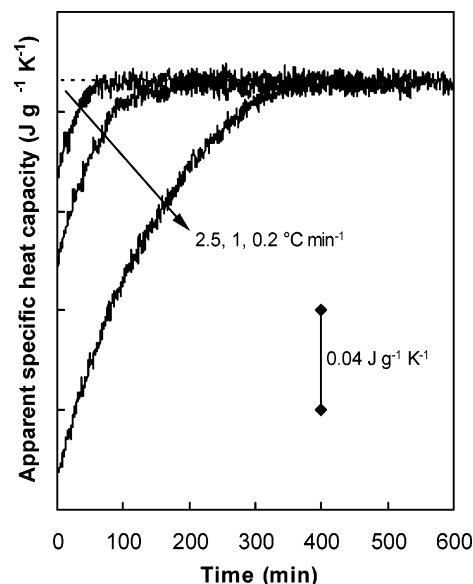


**Figure 7.**  $c_p^{\text{app}}$  during quasi-isothermal remixing at 19 °C for 50/50 PNIPAM 74000/water after heating (demixing) up to 80 °C at different heating/cooling rates: 2.5, 1, and 0.2 °C min<sup>-1</sup>.  $c_p^{\text{base}}$  at 19 °C is indicated (dashed line).

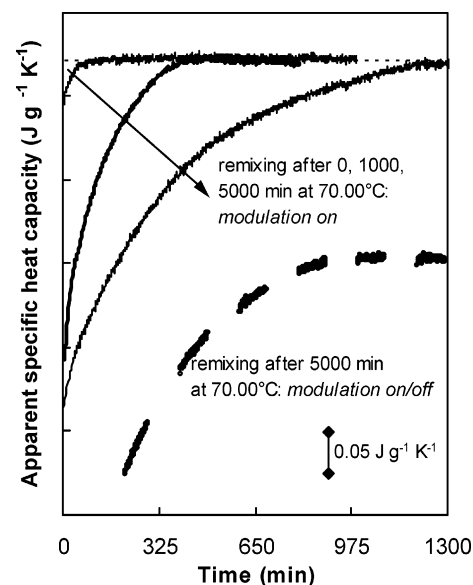


**Figure 8.**  $c_p^{\text{app}}$  during quasi-isothermal remixing at 19 °C for 50/50 PNIPAM 74000/water after heating (demixing) up to 70 °C and different demixing times at 70 °C: 0, 1000, and 5000 min (modulation on), and 5000 min (modulation on/off). The latter curve is shifted by 0.15 J g<sup>-1</sup> K<sup>-1</sup> for clarity.  $c_p^{\text{base}}$  at 19 °C is indicated (dashed line).

line heat capacity  $c_p^{\text{base}}$  (Figure 7), as was also seen for partially miscible polymer blends with interference of vitrification during demixing<sup>26,27</sup> and for the poly(*N*-vinylcaprolactam)/water system.<sup>17</sup> The time needed to completely homogenize the PNIPAM 74000/water sample at 19 °C changes from 90 min (after cooling at 2.5 °C min<sup>-1</sup>) up to 500 min (after cooling at 0.2 °C min<sup>-1</sup>), in agreement with the effect of partial vitrification on the remixing kinetics.

This slowing down of the remixing process is also illustrated in Figure 8. A 50/50 PNIPAM 74000/water mixture was heated to 70 °C and further demixed at 70 °C (zone C) for a period of 0, 1000, and 5000 min. Afterward, the demixed sample was cooled to 19 °C to monitor the return of  $c_p^{\text{app}}$  to  $c_p^{\text{base}}$ . It is clear that the

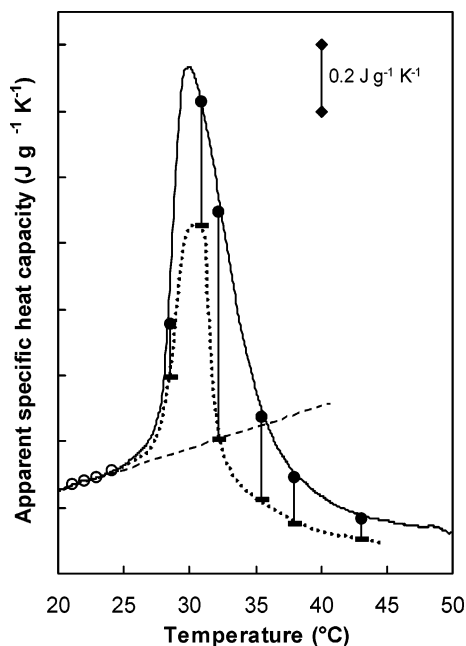


**Figure 9.** Overlay of the evolution in  $c_p^{\text{app}}$  for 50/50 PNIPAM 18000/water: heating curve (demixing); stepwise quasi-isothermal measurements with a step of 1 °C below 24.0 °C (○, equilibrium value); partial quasi-isothermal demixing (28.5, 30.8, 32.2, 35.5, 38.0, and 43.1 °C), starting from a homogeneous mixture at 15.0 °C heated at 1 °C min<sup>-1</sup> to the respective temperatures: time evolution (vertical lines) from start (●) to end (—). Dashed line (extrapolated experimental  $c_p^{\text{base}}$ ) and dotted line (equilibrium  $c_p^{\text{app}}$ ) are a guide to the eye.

lowest initial value in  $c_p^{\text{app}}$  is found for the longest demixing time in zone C due to a higher degree of vitrification of the polymer-rich phase. Furthermore, the initial slope of the remixing curve at 19 °C decreases and the remixing time increases with increasing demixing time. The longest remixing time (ca. 1300 min at 19 °C) is observed for a demixing time of 5000 min at 70 °C. To achieve homogenization of a demixed PNIPAM/water system, water has to diffuse into the polymer-rich phase. The higher the degree of partial vitrification of the polymer-rich phase, the more the kinetics of remixing will be slowed down.

Figure 8 also includes a remixing experiment in which the temperature modulation was periodically switched on and off. Note that the apparent specific heat capacity cannot be measured in the segments where the modulation is turned off. This curve shows an analogous trend as the experiment in which the modulation was always switched on. As such, one can conclude that the observed time-dependent evolutions are not influenced by the applied modulation.

**Quasi-Isothermal Study: Kinetics of Partial Demixing and Remixing of PNIPAM/Water. Time Dependency of the Apparent Heat Capacity.** The time-dependent behavior of the apparent specific heat capacity, determined by means of quasi-isothermal MTDSC experiments, gives additional information on the phase separation kinetics. In Figure 9, stepwise quasi-isothermal measurements are compared with a nonisothermal measurement of  $c_p^{\text{app}}$  for a 50/50 PNIPAM 18000/water solution. At temperatures below the demixing temperature (24.1 °C based on a threshold value of 0.01 J g<sup>-1</sup> K<sup>-1</sup>), no time dependency is noticed. The quasi-isothermal (Figure 9, ○) and the nonisothermal values (Figure 9, continuous line) of  $c_p^{\text{app}}$  coincide,

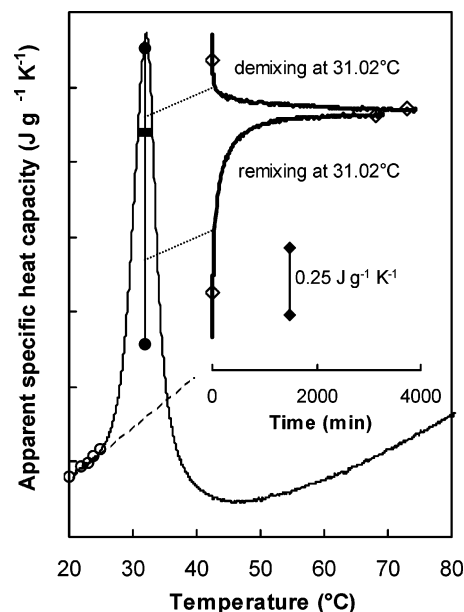


**Figure 10.** Overlay of the evolution in  $c_p^{\text{app}}$  for 50/50 PNIPAM 74000/water: heating curve (demixing); stepwise quasi-isothermal measurements with a step of 1 °C below 24.0 °C (○, equilibrium value); partial quasi-isothermal demixing starting from a homogeneous mixture at 15.0 °C heated at 1 °C min<sup>-1</sup> to 31.02 °C (inset: upper curve) and partial quasi-isothermal remixing starting from a heterogeneous mixture at 45.0 °C (for 2000 min) cooled at 1 °C min<sup>-1</sup> to 31.02 °C (inset: lower curve): time evolution (vertical lines) from start (●) to end (—). Dashed line (extrapolated experimental  $c_p^{\text{base}}$ ) is a guide to the eye. Inset: selected times (◇) for the time domain analysis of Figure 13.

which are therefore considered as baseline specific heat capacities,  $c_p^{\text{base}}$ .

At temperatures above 24.1 °C,  $c_p^{\text{app}}$  is time-dependent until a final excess contribution is attained, as indicated by vertical lines in Figure 9 (start (●), end (—)). This slow evolution, which can take up to 5000 min, is attributed to morphological changes or inter-phase development within the sample. The dotted curve in Figure 9, connecting the measured final values of  $c_p^{\text{app}}$ , shows the magnitude of the remaining excess contribution: the final value of  $c_p^{\text{app}}$  is up to 20% or ca. 0.7 J g<sup>-1</sup> K<sup>-1</sup> higher than the estimated experimental  $c_p^{\text{base}}$ . From this curve it is clear that the drop of  $c_p^{\text{app}}$  below  $c_p^{\text{base}}$  is detected ca. 4 °C sooner for stepwise quasi-isothermal experiments than in the case of heating at 1 °C min<sup>-1</sup>. Note that an analogous effect is seen in Figure 6: the drop of  $c_p^{\text{app}}$  below  $c_p^{\text{base}}$  is detected 2 °C earlier, when the heating rate is lowered from 2.5 to 0.2 °C min<sup>-1</sup>. This heating rate dependence is caused by the kinetics of phase separation and the influence of the partial vitrification process on it,<sup>17</sup> which is even more obvious in the case of partially miscible polymer blends,<sup>26</sup> due to more pronounced diffusion restrictions.

This stepwise quasi-isothermal study was also performed for PNIPAM of other molecular weights. An example is given in Figure 10 for a 50/50 PNIPAM 74000/water solution. The stepwise quasi-isothermal and the nonisothermal values of  $c_p^{\text{app}}$  again coincide (Figure 10, ○) up to the demixing temperature (23.9 °C). At higher temperatures  $c_p^{\text{app}}$  becomes time-dependent, as illustrated at 31.02 °C for both a partial demixing and remixing experiment (Figure 10, start (●), end (—)). The inset in Figure 10 shows that  $c_p^{\text{app}}$  decreases

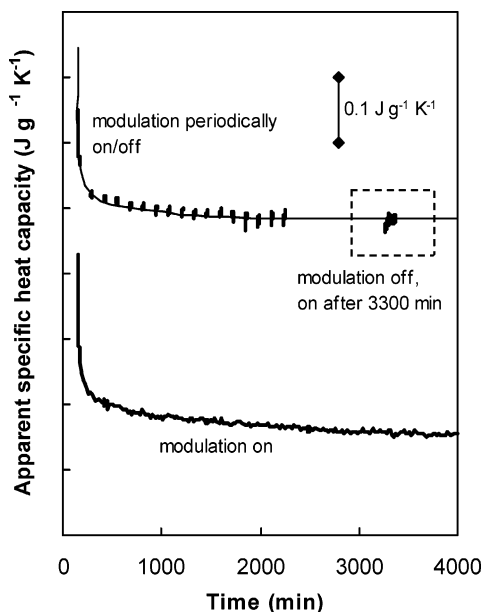


**Figure 11.**  $c_p^{\text{app}}$  during partial quasi-isothermal demixing at 31.02 °C for 50/50 PNIPAM 74000/water, starting from a homogeneous mixture at 15.0 °C heated at 1 °C min<sup>-1</sup> to 31.02 °C: modulation periodically on/off; modulation off, on after 3300 min; and modulation continuously on. The latter curve is shifted by 0.35 J g<sup>-1</sup> K<sup>-1</sup> for clarity. Upper continuous line is a guide to the eye.

when starting from a homogeneous sample (upper curve), whereas it increases toward the same final value when starting from heterogeneous conditions (lower curve). Thus, the final value is only temperature-dependent and independent of the thermal history of the PNIPAM/water sample. This was confirmed by changing the cooling method for the partial remixing experiment; instead of cooling at 1 °C min<sup>-1</sup>, the sample was jump-cooled from 45 °C (after a demixing step of 2000 min). A different evolution in  $c_p^{\text{app}}$  was noticed (not shown); however, the same final value was attained. Moreover, the time dependency at 31.02 °C is not influenced by the temperature modulation itself, as shown in Figure 11 for different on/off sequences of the modulation.

$c_p^{\text{excess}}$  is related to enthalpy changes of demixing and remixing on the time scale of the modulation (see also Time Domain Analysis). MTDSC thus enables, by means of quasi-isothermal heat capacity measurements, to characterize the demixing/remixing reversible processes occurring at the polymer/water interphase of the coexisting phases. The polymer/water fraction participating in this exchange process slowly diminishes toward an equilibrium condition. The observed time dependency over a long time interval can be associated with the diffusion of water molecules within the polymer aggregates and with the specific interactions of these water molecules surrounding the polymer chains. One can conclude that the evolution in  $c_p^{\text{excess}}(T, t)$  is reflecting the progress of phase separation or morphology development (irreversible process).

**Excess Heat Capacity: Effect of the Modulation Period.** One must keep in mind that thus far the discussed results were obtained using standard modulation conditions, i.e., a modulation amplitude of 0.50 °C and a period of 60 s. Changing the modulation sequence, such as periodically on/off, is not influencing the long-term evolution of the polymer/water interphase in zone

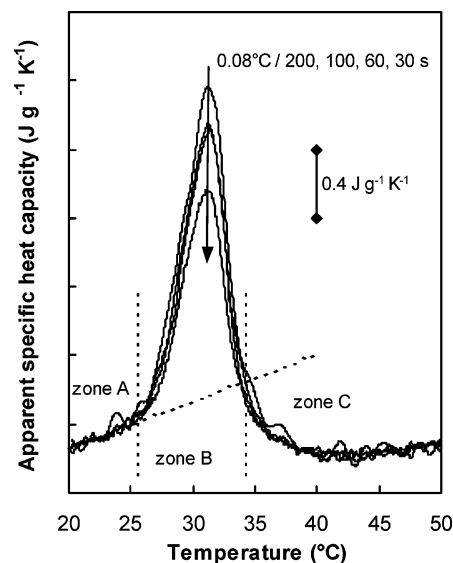


**Figure 12.**  $c_p^{\text{app}}$  during nonisothermal demixing for 40/60 PNIPAM 74000/water at 0.2 °C min<sup>-1</sup>, modulation amplitude of 0.08 °C for periods of 200, 100, 60, and 30 s. Dashed line (extrapolated experimental  $c_p^{\text{base}}$ ) is a guide to the eye.

B, as demonstrated in Figure 11. Changing the modulation parameters, however, will influence the reversible demixing/remixing process at the interphase, which will consequently alter the magnitude of  $c_p^{\text{excess}}$  and  $c_p^{\text{app}}$  in zone B.

Figure 12 shows the variation in  $c_p^{\text{app}}$  for constant amplitude of 0.08 °C and different periods between 200 and 30 s. These experiments were performed on a TA Instruments Q1000 system with advanced T-zero technology in order to obtain a more absolute heat flow and to improve the stability of the average temperature and the amplitude and to expand the range of periods. Hermetic Mettler aluminum pans were used for a more reliable pan/sensor thermal resistance. A smaller heating/cooling rate of 0.2 °C min<sup>-1</sup> was used in order to obtain always at least four modulation cycles during the transition of interest. For a fixed average heating rate and modulation amplitude, smaller modulation periods result in smaller amounts of heat exchanged in one modulation cycle, leading to smaller excess contributions over the entire temperature range in which phase separation occurs. Since the total demixing enthalpy remains constant, the contribution in the nonreversing heat flow increases from 0.33 up to 3.50 J g<sup>-1</sup>, when the period is decreased from 200 to 30 s. This is seemingly in contradiction with results from Cho et al., who stated that upon decreasing the period the heat effect in the nonreversing heat flow became smaller.<sup>13</sup> They also claimed that the single endothermic peak (i.e., the total heat flow) was separated into an endothermic contribution, found in the nonreversing heat flow, and an exothermic contribution, found in the reversing heat flow. This exothermic reversing heat flow, however, is in our opinion erroneous and is most probably caused by an error in a previous software version (wrong sign in the multiplication factor to convert the cyclic heat capacity into the reversing heat flow signal). This error also explains the opposite effect of the modulation period on the nonreversing heat flow. Consequently, the physical interpretation of the exothermic and endothermic heat flow contributions in terms of different hydrophilic and hydrophobic interactions between PNIPAM and the



surrounding water molecules no longer holds. In our opinion, only endothermic contributions, in both the reversing and nonreversing heat flow, are seen for all modulation conditions during demixing (on heating) whereas only exothermic contributions are noticed for the remixing process (on cooling). This conclusion is valid for poly(vinylcaprolactam)/water,<sup>17</sup> PNIPAM/water (this work), and poly(vinyl methyl ether)/water,<sup>16</sup> representing type I, II, and III LCST phase separation behavior, respectively.<sup>15</sup> MTSDC does not allow to distinguish different specific interactions (such as hydrogen bonding and hydrophobic associations) in separate exothermic and endothermic heat flow contributions but is an excellent analytical tool to study the kinetics of the demixing and remixing processes in these polymer/water systems both on a molecular (fast reversible process in the polymer/water interphase) and a macroscopic level (slow evolution of morphology).<sup>16,17</sup>

In the case of mobility restrictions due to the interfering partial vitrification of the PNIPAM-rich phase in zone C, no or at most a very small excess contribution is expected. Figure 12 confirms that the modulation period has a negligible effect on  $c_p^{app}$  in zone C (beyond 35 °C): only the frequency dependency of the partially vitrified PNIPAM phase is seen (small effect).

**Time Domain Analysis.** The time evolution in  $c_p^{app}$  and the equilibrium state itself can be analyzed in a quantitative manner by considering the raw modulated heat flow signal as a function of time. This time domain analysis was previously introduced for studying reversible processes at the melting temperature of indium<sup>30</sup> and in the melting region of poly(ethylene oxide).<sup>31</sup> Recently, it has been explored for studying phase separation kinetics of the poly(vinyl methyl ether)/water system.<sup>16</sup>

Figure 10 shows that the largest equilibrium value of  $c_p^{app}$  occurs at about 31.02 °C. Therefore, this temperature was chosen to perform the time domain analysis for the 50/50 PNIPAM 74000/water system. The stability of the isothermal temperature is of great importance since small variations cause considerable variations of  $c_p^{app}$  in the phase separation region. In the Q1000 system with advanced T-zero technology, the applied constant temperature and the temperature amplitude are remarkably stable (within  $\pm 0.002$  and  $\pm 0.0001$  °C, respectively, for 1000 min).

Figure 13 shows the result of a time domain analysis for two modulation periods at 31.02 °C. Standard modulation conditions of 0.50 °C per 60 s were used to clearly show the evolution of the modulated heat flow as well as the excess contribution to the modulated heat flow at two selected times of the partial demixing and remixing measurement (selected times are indicated in the inset of Figure 10 ( $\diamond$ )). Figure 13a depicts the measured modulated heat flow (thin), the reference signal (thick), and the difference between both signals, which is the excess contribution (shaded areas) at the final value of  $c_p^{app}$  in the demixing experiment at 31.02 °C (Figure 10, inset: upper curve at  $t = 3850$  min). The reference signal is constructed using the extrapolated baseline at 31.02 °C.

Two corrections were made to the raw modulated heat flow.<sup>16</sup> First, an instrument heat flow phase correction has been applied by considering the heat flow phase from outside the transition region. In this way only contributions arising from sample transitions will show up. As a second correction, a small heat flow shift is

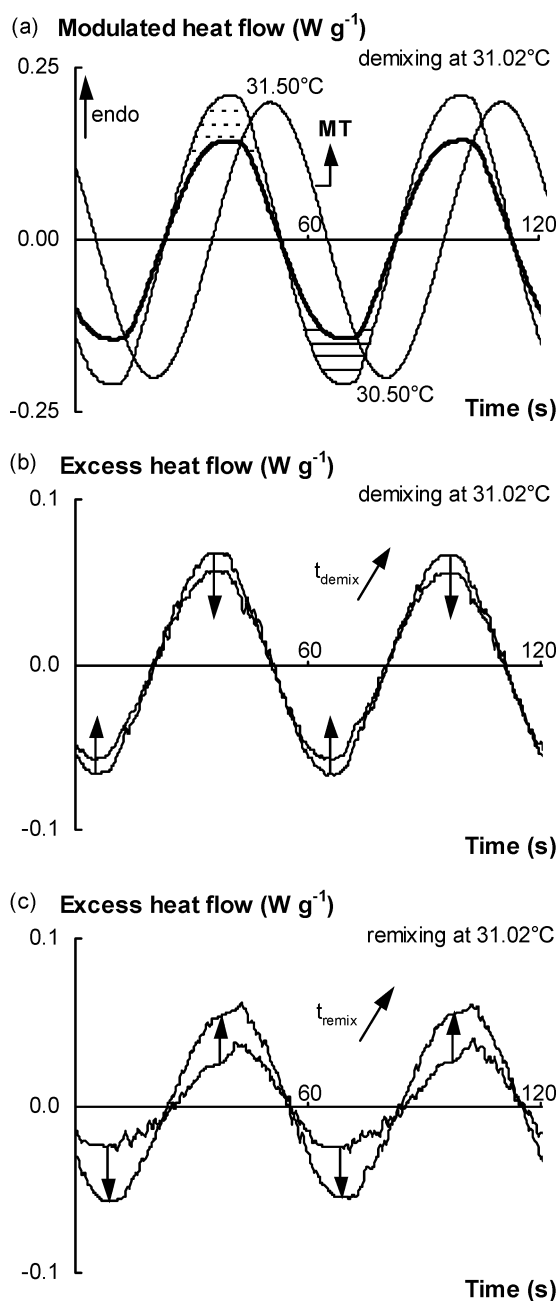


**Figure 13.** (a) Two modulation periods of 60 s of the corrected modulated heat flow (thin) and reference modulated heat flow (bold). The shaded areas represent the excess contribution: exothermic (—) and endothermic (---). The modulated temperature (MT,  $\pm 0.50$  °C around 31.02 °C) is shown for comparison with the modulated heat flow. (b) Time evolution of the excess heat flow at selected times depicted in the inset of Figure 10 ( $\diamond$ , upper curve). Quasi-isothermal demixing at 31.02 °C after heating a homogeneous mixture from 15 °C at 1 °C min<sup>-1</sup>. (c) Time evolution of the excess heat flow at selected times depicted in the inset of Figure 10 ( $\diamond$ , lower curve). Quasi-isothermal remixing at 31.02 °C after cooling a heterogeneous mixture from 45 °C at 1 °C min<sup>-1</sup>.

performed in order to attain equal contributions of endothermic and exothermic effects in the modulated heat flow signal for (time-independent) baseline conditions, e.g., at 10 °C. At this temperature no heat effects occur due to demixing/remixing, and thus only  $c_p^{base}$  is measured. The same shift has been applied in all temperature regions of interest.

The modulated temperature (MT) is also shown in Figure 13a, indicating the reversibility of the demixing/



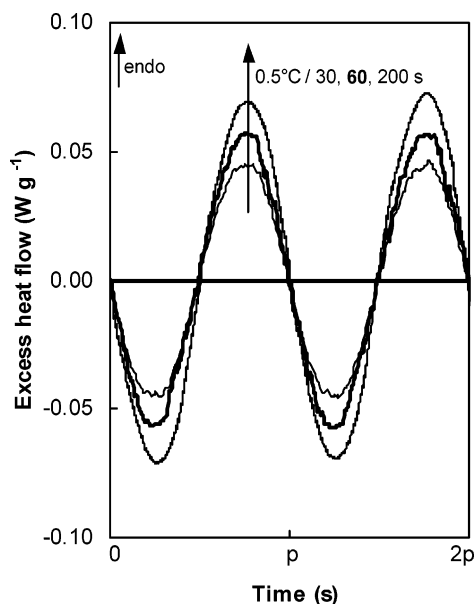


**Figure 14.** Effect of the modulation period  $p$  on the final excess heat flow after partial quasi-isothermal demixing at 31.02 °C for 50/50 PNIPAM 74000/water.

remixing process on the time scale of the modulation (60 s). Raising the temperature introduces endothermic excess contributions, coupled with demixing, while cooling leads to exothermic excess contributions, coupled with remixing.

Parts b and c of Figure 13 depict the excess heat flow for two selected times of the partial demixing and remixing measurement, respectively. The evolutions in the excess heat flow correspond to the evolutions in  $c_p^{\text{app}}$ , as shown in the inset of Figure 10: endothermic and exothermic heat effects decrease when starting from a homogeneous mixture (Figure 13b), and they increase when an initially heterogeneous mixture is partially remixed (Figure 13c). For each intermediate state, the endothermic and exothermic contributions remain equal within experimental error, showing the reversibility of the exchange process as a function of the demixing/remixing time. At the final state of the evolution, an equilibrium excess contribution is reached. By integrating the endothermic and exothermic heat effects in one modulation cycle for the different demixing/remixing times, heat effects on the order of 1 J g<sup>-1</sup> are found for an amplitude of 0.50 °C.

The effect of the modulation period  $p$  on the final excess heat flow after partial quasi-isothermal demixing at 31.02 °C is shown in Figure 14. For a constant amplitude of 0.50 °C, the excess contribution is increasing with the period while the reversibility of the demixing/remixing process is maintained (at least for periods between 30 and 200 s). In the PNIPAM/water system with type II LCST demixing behavior, no clear deformations in the raw modulated heat flow are noticed (see Figures 13 and 14), so  $c_p^{\text{app}}$  ( $c_p^{\text{excess}}$ ) gives quantitative results to a good approximation. In the poly(vinyl methyl ether)/water system, on the contrary, the time domain analysis in the demixing region showed clear distortions in the raw modulated heat flow due to the special aspect of the type III LCST demixing behavior with an interfering three-phase equilibrium.<sup>16</sup>

The frequency dependency of the final value of  $c_p^{\text{excess}}$  at 31.02 °C is further illustrated in Figure 15.  $c_p^{\text{excess}}$  is first increasing with the modulation period, after which

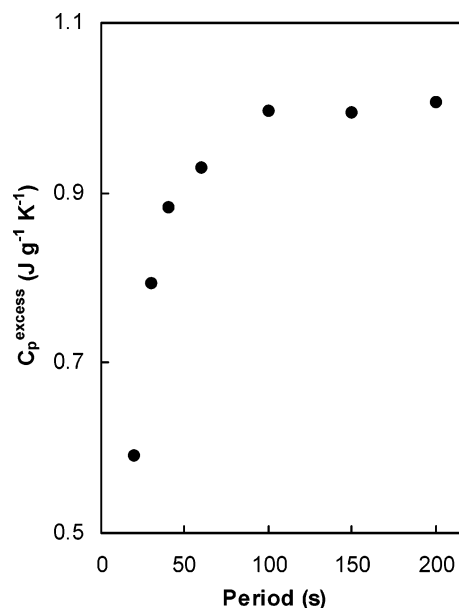


**Figure 15.** Effect of the modulation period (●, fixed amplitude of 0.50 °C) on the final value of  $c_p^{\text{excess}}$  at 31.02 °C for 50/50 PNIPAM 74000/water.

it is leveling off. From ca. 100 s on, an almost constant value of  $c_p^{\text{excess}}$  is observed. In these modulation conditions, the demixing/remixing process in the PNIPAM/water interphase is fast enough to get frequency-independent.

## Conclusions

Modulated temperature DSC has been used to study the LCST behavior and the phase separation kinetics of PNIPAM/water solutions over the entire composition range. The type II LCST demixing behavior has been confirmed, using the specific heat capacity signal in nonisothermal conditions. This signal contains heat effects coupled with demixing and remixing due to reversible processes taking place on the time scale of the modulation (excess contribution,  $c_p^{\text{excess}}$ ), causing the heat capacity to be apparent ( $c_p^{\text{app}}$ ). A distinction between different specific interactions of importance during phase separation, such as hydrogen bonding and hydrophobic associations among PNIPAM and the surrounding water molecules, cannot be made in terms of both heat flow contributions. For all modulation frequencies studied, both reversing and nonreversing heat flows are endothermic for demixing (and exothermic for remixing). MTDSC, however, gives valuable kinetic information on the phase separation process.

The smaller value of  $c_p^{\text{excess}}$  found upon cooling indicates that remixing is slower than demixing. This effect is enlarged by the partial vitrification of the PNIPAM-rich phase, which is usually not taken into account for polymer/water mixtures. However, a higher degree of partial vitrification will increase the remixing time from less than 1 h up to 1 day or even more, indicating the importance of this phenomenon with respect to applications. A higher polymer concentration is slowing down the rate of phase separation as well.

The time dependency of  $c_p^{\text{app}}$  ( $c_p^{\text{excess}}$ ), measured quasi-isothermally in the phase separation region, in combination with a time domain analysis provides additional kinetic information on the fast demixing/remixing processes in the PNIPAM/water interphase and on the slow

evolution of this interphase fraction toward an equilibrium condition, which is independent of the thermal history. The slow morphology development, related to the change in hydration structure surrounding the polymer chains, can take up to several days. This kinetic information is important for the applicability of PNIPAM or other thermoresponsive water-soluble polymers and hydrogels.

**Acknowledgment.** Kurt Van Durme thanks the Flemish Institute for the Promotion of Innovation through Science and Technology in Flanders (I.W.T.) for a Ph.D. grant. Guy Van Assche is a postdoctoral fellow of the Foundation for Scientific Research (Flanders-Belgium).

## References and Notes

- (1) Galaev, I. Y.; Mattiasson, B. *Tibtech* **1999**, *17*, 335–340.
- (2) Choi, Y.; Yamaguchi, T.; Nakao, S. *Ind. Eng. Chem. Res.* **2000**, *39*, 2491–2495.
- (3) Varghese, S.; Lele, A. K.; Mashelkar, R. A. *J. Chem. Phys.* **2000**, *112*, 3063–3070.
- (4) Yamamoto, I.; Iwasaki, K.; Hirotsu, S. *J. Phys. Soc. Jpn.* **1989**, *58*, 210–215.
- (5) Wang, X.; Qiu, X.; Wu, C. *Macromolecules* **1998**, *31*, 2972–2976.
- (6) Gorelov, A. V.; Du Chesne, A.; Dawson, K. A. *Physica A* **1997**, *240*, 443–452.
- (7) Schild, H. G. *Prog. Polym. Sci.* **1992**, *17*, 163–249.
- (8) Lin, S.-Y.; Chen, K.-S.; Run-Chu, L. *Polymer* **1999**, *40*, 2619–2624.
- (9) Ramon, O.; Kesselman, E.; Berkovici, R.; Cohen, Y.; Paz, Y. *J. Polym. Sci., Part B: Polym. Phys.* **2001**, *39*, 1665–1677.
- (10) Ohta, H.; Ando, I.; Fujishige, S.; Kubota, K. *J. Polym. Sci., Part B: Polym. Phys.* **1991**, *29*, 963–968.
- (11) Boutris, C.; Chatzi, E. G.; Kiparissides, C. *Polymer* **1997**, *38*, 2567–2570.
- (12) Heskins, M.; Guillet, J. E. *J. Macromol. Sci., Chem.* **1968**, *2*, 1441–1455.
- (13) Cho, E. C.; Lee, J.; Cho, K. *Macromolecules* **2003**, *36*, 9929–9934.
- (14) Afroze, F.; Nies, E.; Berghmans, H. *J. Mol. Struct.* **2000**, *554*, 55–68.
- (15) Šolc, K.; Dušek, K.; Koningsveld, R.; Berghmans, H. *Collect. Czech. Chem. Commun.* **1995**, *60*, 1661–1688.
- (16) Swier, S.; Van Durme, K.; Van Mele, B. *J. Polym. Sci., Part B: Polym. Phys.* **2003**, *41*, 1824–1836.
- (17) Van Durme, K.; Verbrugghe, S.; Du Prez, F.; Van Mele, B. *Macromolecules* **2004**, *37*, 1054–1061.
- (18) Ricka, J.; Meewes, M.; Nyffenegger, R.; Binkert, T. *Phys. Rev. Lett.* **1990**, *65*, 657–660.
- (19) Reading, M.; Luget, A.; Wilson, R. *Thermochim. Acta* **1994**, *238*, 295–307.
- (20) Wunderlich, B.; Jin, Y.; Boller, A. *Thermochim. Acta* **1994**, *238*, 277–293.
- (21) Reading, M. *Trends Polym. Sci.* **1993**, *8*, 248–253.
- (22) Van Assche, G.; Van Hemelrijck, A.; Rahier, H.; Van Mele, B. *Thermochim. Acta* **1995**, *268*, 121–142.
- (23) Swier, S.; Van Mele, B. *J. Polym. Sci., Part B: Polym. Phys.* **2003**, *41*, 594–608.
- (24) Swier, S.; Van Mele, B. *Macromolecules* **2003**, *36*, 4424–4435.
- (25) Minakov, A. A.; Schick, C. *Thermochim. Acta* **1999**, *330*, 109–119.
- (26) Dreezen, G.; Groeninckx, G.; Swier, S.; Van Mele, B. *Polymer* **2001**, *42*, 1449–1459.
- (27) Swier, S.; Pieters, R.; Van Mele, B. *Polymer* **2002**, *43*, 3611–3620.
- (28) Swier, S.; Van Mele, B. *Polymer* **2003**, *44*, 2689–2699.
- (29) Baltes, T.; Garret-Flaudy, F.; Freitag, R. *J. Polym. Sci., Part A: Polym. Chem.* **1999**, *37*, 2977–2989.
- (30) Ishikiriyama, K.; Wunderlich, B. *J. Polym. Sci., Polym. Phys.* **1997**, *35*, 1877–1886.
- (31) Baur, H.; Wunderlich, B. *J. Therm. Anal. Calorim.* **1998**, *54*, 437–465.

MA048472B